

## Evaluation of corrosion resistance and biocompatibility test of Ti10Mo8Nb alloy for biomedical applications

Avaliação da resistência à corrosão e biocompatibilidade da liga Ti10Mo8Nb para aplicações biomédicas

Evaluación de la resistencia a la corrosión y biocompatibilidad de la aleación Ti10Mo8Nb para aplicaciones biomédicas

Received: 04/24/2025 | Revised: 05/01/2025 | Accepted: 05/02/2025 | Published: 05/04/2025

### **Edwin G. M. Bejarano**

ORCID: <https://orcid.org/0009-0001-2086-8494>  
Federal University of Itajubá, Brazil  
E-mail: [edwinmedinabejarano@unifei.edu.br](mailto:edwinmedinabejarano@unifei.edu.br)

### **Patricia Capellato**

ORCID: <https://orcid.org/0000-0002-6397-5820>  
Federal University of Itajubá, Brazil  
E-mail: [pat\\_capellato@yahoo.com.br](mailto:pat_capellato@yahoo.com.br)

### **Roberto Z. Nakazato**

ORCID: <https://orcid.org/0000-0001-7897-1905>  
University Estadual Paulista "Júlio de Mesquita Filho", Brazil  
E-mail: [roberto.zenhei@unesp.br](mailto:roberto.zenhei@unesp.br)

### **Kerolene B. da Silva**

ORCID: <https://orcid.org/0000-0002-1524-5567>  
University Estadual Paulista "Júlio de Mesquita Filho", Brazil  
E-mail: [kerolene.barboza@gmail.com](mailto:kerolene.barboza@gmail.com)

### **João P. A. Carobolante**

ORCID: <https://orcid.org/0000-0002-5648-6148>  
University Estadual Paulista "Júlio de Mesquita Filho", Brazil  
E-mail: [pedro.carobolante@unesp.br](mailto:pedro.carobolante@unesp.br)

### **Thierre Capellato**

ORCID: <https://orcid.org/0009-0001-7387-5831>  
University Estadual Paulista "Júlio de Mesquita Filho", Brazil  
E-mail: [thierrecapellato@yahoo.com.br](mailto:thierrecapellato@yahoo.com.br)

### **Mirian de L. N. M. Melo**

ORCID: <https://orcid.org/0000-0001-9668-7799>  
Federal University of Itajubá, Brazil  
E-mail: [mirianmottamelo@unifei.edu.br](mailto:mirianmottamelo@unifei.edu.br)

### **Ana Paula R. Alves**

ORCID: <https://orcid.org/0000-0003-3353-4247>  
University Estadual Paulista "Júlio de Mesquita Filho", Brazil  
E-mail: [paula.rosifini@unesp.br](mailto:paula.rosifini@unesp.br)

### **Daniela Sachs**

ORCID: <https://orcid.org/0000-0002-3767-2455>  
Federal University of Itajubá, Brazil  
E-mail: [danisachs@unifei.edu.br](mailto:danisachs@unifei.edu.br)

### **Abstract**

Among the various materials used in the composition of biomedical implants, titanium alloys (Ti) stand out, mainly the  $\beta$ -phase ternary alloys. The Ti10Mo8Nb alloy developed in an electric arc furnace and rotary forging was analyzed and showed adequate mechanical properties. However, its corrosion resistance has not been deeply investigated in the literature. This research aims to investigate the corrosion resistance and bacterial proliferation of  $\beta$ -phase alloys composed of titanium, molybdenum and niobium (Ti10Mo8Nb). For corrosion analysis, a passive current density of  $4.2 \cdot 10^{-5}$  A/cm<sup>2</sup> and a dissolution potential of 1.5 V were obtained. Its biocompatibility tests, based on bacterial proliferation was 12.3% lower than that of commercially pure Ti. Combined with the mechanical characteristics of Ti10Mo8Nb, the alloy presented potential and advantageous properties to make it applicable in the field of biomedical application.

**Keywords:** Titanium alloy; Corrosion resistance; Bacterial proliferation; Biomedical application; Ti10Mo8Nb alloy.

### Resumo

Dentre os diversos materiais utilizados na composição de implantes biomédicos, destacam-se as ligas de titânio (Ti), principalmente as ligas ternárias de fase  $\beta$ . A liga Ti10Mo8Nb desenvolvida em forno elétrico a arco e forjamento rotativo foi analisada e apresentou propriedades mecânicas adequadas. Entretanto, sua resistência à corrosão ainda não foi profundamente investigada na literatura. Esta pesquisa tem como objetivo investigar a resistência à corrosão e à proliferação bacteriana de ligas de fase  $\beta$  compostas por titânio, molibdênio e nióbio (Ti10Mo8Nb). Para análise de corrosão, obteve-se uma densidade de corrente passiva de  $4,2 \cdot 10^{-5}$  A/cm<sup>2</sup> e um potencial de dissolução de 1,5 V. Seus testes de biocompatibilidade, baseados na proliferação bacteriana, foram 12,3% inferiores aos do Ti comercialmente puro. Aliada às características mecânicas do Ti10Mo8Nb, a liga apresentou potencial e propriedades vantajosas para torná-la aplicável no campo de aplicação biomédica.

**Palavras-chave:** Liga de titânio; Resistência à corrosão; Proliferação bacteriana; Aplicação biomédica; Liga Ti10Mo8Nb.

### Resumen

Entre los diversos materiales utilizados en la composición de implantes biomédicos, destacan las aleaciones de titanio (Ti), principalmente las ternarias de fase  $\beta$ . La aleación Ti10Mo8Nb, desarrollada en horno de arco eléctrico y forjado rotatorio, fue analizada y mostró propiedades mecánicas adecuadas. Sin embargo, su resistencia a la corrosión no se ha investigado a fondo en la literatura. Esta investigación tiene como objetivo investigar la resistencia a la corrosión y la proliferación bacteriana de aleaciones de fase  $\beta$  compuestas de titanio, molibdeno y niobio (Ti10Mo8Nb). Para el análisis de corrosión, se obtuvo una densidad de corriente pasiva de  $4,2 \cdot 10^{-5}$  A/cm<sup>2</sup> y un potencial de disolución de 1,5 V. Sus pruebas de biocompatibilidad, basadas en la proliferación bacteriana, fueron un 12,3 % inferiores a las del Ti comercialmente puro. En combinación con las características mecánicas del Ti10Mo8Nb, la aleación presentó propiedades potenciales y ventajosas que la hacen aplicable en el campo de las aplicaciones biomédicas.

**Palabras clave:** Aleación de titanio; Resistencia a la corrosión; Proliferación bacteriana; Aplicación biomédica; Aleación Ti10Mo8Nb.

## 1. Introduction

The expansion of access to orthopedic and dental implants observed in recent years brings direct benefits to the patients' quality of life and recovery from chronic or emergency illnesses. On the other hand, it presents a challenge with a progressive impact measured in terms of financial resources and technological advances for global health systems. Some social elements explain the importance of implants and their high demand: increased life expectancy; change in the proportion between the elderly and young population observed in several countries; increase in the number of bone fractures that have occurred in the last twenty years. Thus, the search for materials that pre-sent greater resistance for long-term applications and better biocompatible response is constant in the scientific and industrial communities (Gu & Dupre, 2021; Gericke et al., 2021; Guo et al., 2022; Dixon, 2022; Dogra, et al., 2022).

Among the various materials used in the composition of implants, titanium alloys (Ti) stand out, mainly the  $\beta$ -phase ternary alloys. Such alloys have a lower modulus of elasticity, reducing protection against stress as this parameter approaches the natural value of the bone, and greater resistance to corrosion (Toledona- Serrabona et al., 2021). In general, the Young's modulus of titanium varies from 100 to 150 GPa. Although it is a higher value than that observed in bones (10-30 GPa), it is more appropriate than the elastic modulus of other alloys, such as those composed of stainless steel and CoCrMo, which can reach values greater than 500 GPa (Chelariu, 2014). This type of alloy for the medical field has an estimated market of 45.5 billion dollars for medical products made from titanium (Li et al., 2021). Likewise, more than 330,000 patients annually receive bone hip implants in the United States alone, making it one of the most common surgical procedures (Royhman et al., 2021). The performance of dental bone replacement procedures is expected to grow by 9.5% per year, at least until 2025 (Zhao et al., 2021). And these numbers are expected to increase even further, as the population aged 65 and over is expected to increase by 20% by 2050, making this group more vulnerable to orthopedic fractures or dental problems. (Massari et al., 2019).

Although Ti alloys have significant relevance for healthcare solutions, biochemical aspects related to the human body can lead to material wear. Depending on the characteristics of the surface and the constituent elements, the body's action on the

implant can lead to corrosion and the consequent release of particles. These particles can affect the functionality of the implant, altering its mechanical behavior and bone resorption. Furthermore, indirectly, it can lead to blood contamination and adverse problems with the patient's immune or neurological system. Regardless of the composition of Ti alloys, the change in its composition affects properties related to genotoxicity and cytotoxicity in a positive or negative way (Apiwantanakul & Chantarawatit, 2021; Montiel-Flores et al., 2021).

For example, Ti6Al4V alloys have become widely applied due to their mechanical properties suitable for bone implants. However, several studies indicate that its composition of aluminum (Al) and vanadium (V) is correlated with inflammatory processes and neurological disorders, such as Alzheimer's disease (Montiel-Flores et al., 2021). On the other hand, the use of niobium (Nb) and molybdenum (Mo) in the alloy can increase the microhardness of the implant, as well as reduce its porosity and elastic modulus. Thus, in a previous work, a new  $\beta$ -phase alloy composed of titanium, molybdenum and niobium (Ti10Mo8Nb) developed using an electric arc furnace and rotary forging was analyzed. This alloy had an elastic modulus of  $91 \pm 1$  GPa, lower than the modulus of pure Ti ( $108 \pm 4$  GPa) and Ti6Al4V ( $113 \pm 10$  GPa). Furthermore, it presented a microhardness of 343.4 HV, higher than that presented by pure Ti and other titanium alloys (e.g. Ti6Al4V, Ti15Mo, Ti7.5Mo), which is an important characteristic to avoid failures in articulated implants. (Capellato et al., 2022).

Thus, the search for materials that present corrosion resistance, biocompatibility and adequate mechanical properties is a recurring theme in literature and is valuable for the advancement of biomaterials used in orthopedic and dental implants. This research aims to investigate the corrosion resistance and bacterial proliferation of  $\beta$ -phase alloys composed of titanium, molybdenum, and niobium (Ti10Mo8Nb).

## 2. Methodology

A laboratory research was carried out, of a qualitative and quantitative nature (Pereira et al., 2018; Gil, 2017).

### 2.1 Alloy processing of the alloy

Ti10Mo8Nb alloy (mass fraction in%) was prepared by mixing an appropriate amount of high purity sponge Ti (Sandinox, 99.8%), Mo (Sigma-Aldrich, 99.9%), and Nb (Sandinox, 99.9 %). The mixtures were melted under a high-purity argon atmosphere in a vacuum non-consumable arc melting furnace. The ingots were inverted and re-melted at least four times to maintain homogenization. The alloy was homogenized in vacuum at 1000°C for 24 hours and solubilized at 950°C for 1 hour and quenched in water. After heat treatment, the ingot was cold worked by a rotary stamping process until it reached a diameter of 10 mm. The ingots were cleaned with water, neutral soap and acetone and, again, solubilized at 950 °C for 1 hour and quenched in water to ensure the presence of the  $\beta$  phase. Finally, they were polished on 1200 mesh sandpaper and cleaned in an ultrasonic bath with soap and water (20 min), deionized water (20 min) and isopropyl alcohol (5 min).

### 2.2 Electrochemical Corrosion Resistance Tests

The circular surface exposed to attack during the test had a diameter of 6 mm. For each test, 125 ml of Fetal Bovine Serum solution (FBS, Sigma-Alrich) was used at an initial temperature of 25.5°C, 1 platinum working electrode, 2 platinum counter electrodes and 1 Ag/AgCl reference electrode.

The electrochemical behavior of the Ti10Mo8Nb alloy was investigated in a naturally aerated solution, 125 ml, containing fluoride and chloride ions. The samples (working electrode) were sanded with sandpaper up to 600 mesh, cleaned with deionized water and dried in the open air. The surface area of the working electrode was 1.0 cm<sup>2</sup>. A saturated calomel electrode (Ag/AgCl in saturated KCl solution) was used as the reference electrode and a platinum foil as the counter electrode.

The composition of the solution used in the corrosion tests was: NaCl 0.15 mol/L and NaF 0.03 mol/L, the pH of the solution was adjusted to 6.0. The temperature of the electrochemical cell was maintained at  $37 \pm 0.1$  °C.

Electrochemical measurements were performed using an EG&G potentiostat/galvonostat instrument, model 238 (Princeton Applied Research, USA), controlled by a personal computer and Electro-chemistry Power Suite software (version 2.0, Ametek Inc.).

The Ti10Mo8Nb alloy samples were immersed in the solution for 3 hours to stabilize the open circuit potential value. Afterwards, potentiodynamic polarization tests began with a potential sweep rate of 1 mV/s, from -0.67 to 3.00 V versus Ag/AgCl in order to investigate the behavior of passive layer. The electrochemical tests were repeated twice (test 01 and test 02) to ensure the reproducibility of the measurements.

### 2.3 Micrography Evaluation

The characterization of the samples' surfaces was carried out using a scanning electron micro-scope (SEM). The SEM images were obtained with an accelerating voltage of 10.0 kV. The SEM equipment used was the Shimadzu SS-550.

### 2.4 Bacteria Proliferation Test

For the experiment, strains of *Staphylococcus aureus* (ATCC 6538) and *Staphylococcus epidermidis* (ATCC 12228) were used. Initially, BHI media - sterile solution for brain and heart infusion - were prepared, using 52 g of BHI diluted in 1000 mL of distilled water. The BHI solution was sterilized in an autoclave at 127 °C for a period of 1 h. After this procedure, the strain was inoculated in a test tube with 3 mL of BHI and placed in an oven at 37 °C for 24 hours (performed in duplicate). After the incubation period, 10 µL of the solution prepared with the strain was used to seed the Petri dishes previously prepared with agar. The plates were taken to a bacteriological oven at 37 °C for a period of 24 hours for biofilm growth. Finally, an aliquot of the cultured bacterial colony was added to a test tube with 3 mL of 0.9% NaCl solution until the concentration of the liquid medium was on the 0.5 McFarland scale ( $1.5 \times 10^8$  cells/ mL).

To carry out the test, a total of 10 samples were used, which were divided into two groups, the control group with five coated Ti10Mo8Nb samples and the test group, where five Ti10Mo8Nb samples were coated. GT samples were UV sterilized for 30 minutes. Then, samples from both groups were placed in a well plate and covered with 3 mL of BHI and 100 µL of 0.5 McFarland suspension was added to each well. Again, the plates were placed in an oven at 37°C for 48 hours.

After the incubation period, the samples were placed in test tubes with 3 mL of saline solution, vortexed for 3 minutes and washed in ultrasound for a period of 10 minutes, thus dispersing the biofilms formed to generate a pure bacterial solution. From this solution, five dilutions were made (pure, 10<sup>-2</sup>, 10<sup>-4</sup>, 10<sup>-6</sup> and 10<sup>-8</sup>) in 0.9% saline solution. Subsequently, one drop of each dilution was inoculated into a Petri dish prepared with agar and, finally, the plates were placed in an oven at 37°C for 24h. At the end of the process, the growth of colonies on the surface of the plates was verified. The results obtained were log<sub>10</sub> transformed and analyzed by Student's T test. The calculation was performed using the GraphPad Prism software. P<0.05 was considered to indicate a statistically significant difference between coated and uncoated samples.

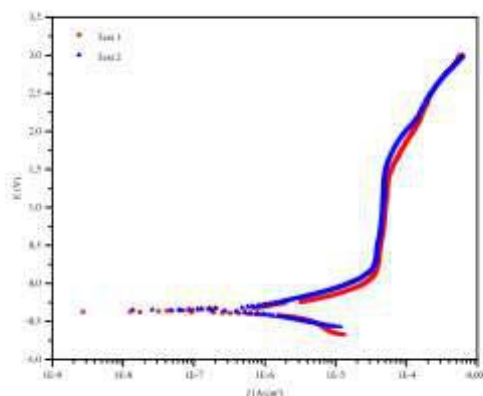
## 3. Results and Discussion

Thus, based on the established methodology, tests were carried out for subsequent analysis. The importance of evaluating the corrosion of the alloy is highlighted, as well as the characterization of its bacterial proliferation as a way of allowing the use of more suitable materials in the formulation of biomedical application.

As for the electrochemical corrosion resistance test, after 3 hours of immersion of the Ti10Mo8Nb samples in the

solution, there was no clear stabilization of the potential. Even so, the final potentials recorded were used to establish the range used in the potentiodynamic polarization. The two curves presented a relatively close open circuit potential (OCP) value. Test 01 with -0.37 V, test 02 with -0.27 V and an average of -0.32 V. The Potentiodynamic Polarization (Figure 1) drawn from the data obtained by potentiodynamic analysis allows observing some parameters that allow a deeper description of the electrochemical behavior of the material, such as the cathodic and anodic regions, the corrosion potential and current, the presence of a passivation region of the material, and consequently, the passivation current density and the primary corrosion potential. In a simple way, we can evaluate these data as follows, the lower the corrosion density, the lower the corrosion rate, and therefore, the more resistant the material.

**Figure 1** - Electrochemical behavior for corrosion resistance analysis of the alloy for two tests (blue and red lines).

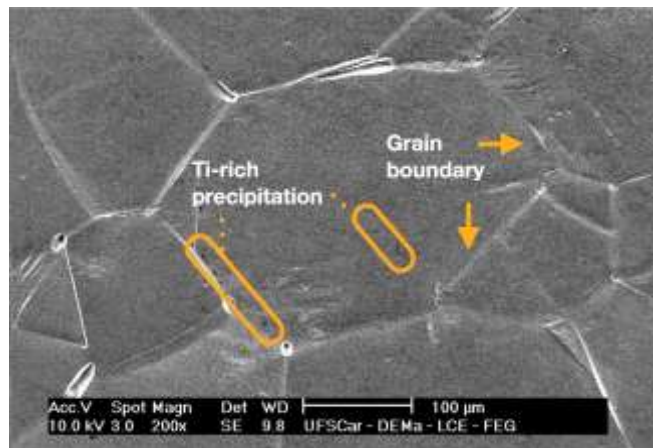


Source: Authors.

The curves obtained in the two tests presented a similar profile, with the same corrosion potential values, -0.37 V and corrosion current density of  $2.3 \cdot 10^{-6}$  A/cm<sup>2</sup> and  $8.5 \cdot 10^{-7}$  A/cm<sup>2</sup> for tests 01 and 02, respectively. The corrosion potentials obtained were close to those found by the OCP curves, revealing that they were close to stabilization of the curve after 3 hours of immersion. In both curves, there is the formation of a passive region, characteristic of titanium and its alloys. In test 01, the passive current density is  $4.2 \cdot 10^{-5}$  A/cm<sup>2</sup> and the dissolution potential is 1.5 V. In test 02, values very close to the first test,  $4.3 \cdot 10^{-5}$ , are observed. A/cm<sup>2</sup> and 1.5 V.

In the micrograph obtained in SEM (Figure 2), it is possible to observe that the sample has a typically equiaxed crystalline structure, with an average grain size of approximately 150  $\mu$ m.

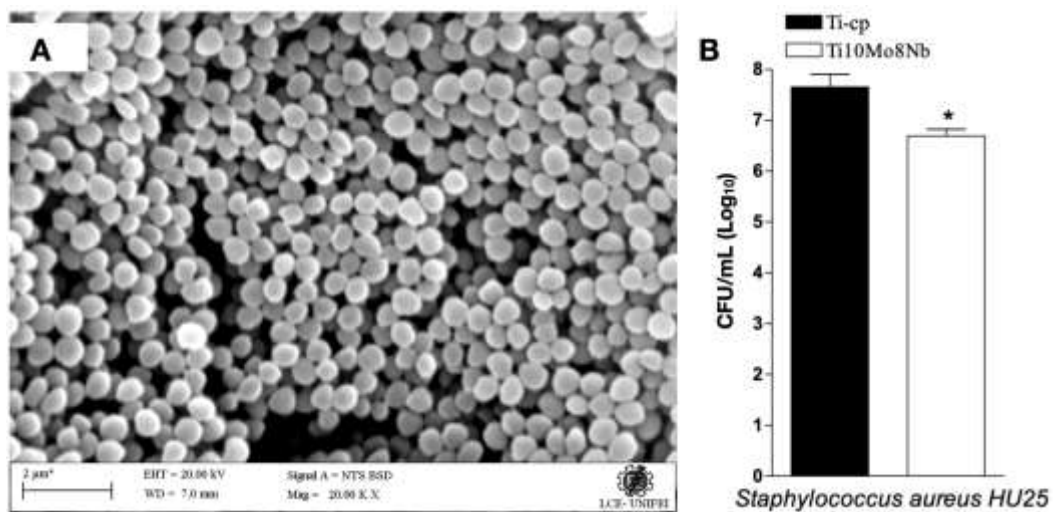
**Figure 2** - Micrograph of the alloy demonstrating equiaxed structure and Ti-rich precipitation.



Source: Authors.

The evaluation of the adhesive behavior of bacteria was carried out on the surface of the Ti10Mo8Nb and Ti-cp alloy. In this investigation, Ti-cp showed a higher concentration of colony forming units (CFU) when compared to Ti10Mo8Nb, as shown in Figure 3.

**Figure 3** - Concentration of colony forming units (CFU) for Ti-cp and Ti10Mo8Nb samples, (A) SEM image with colonies formed on the Ti10Mo8Nb sample and (B) CFU/mL graph for *Staphylococcus aureus*.



Source: Authors.

Ti10Mo8Nb showed a 12.3% reduction in CFU. In this case, an SEM image was recorded to represent the units formed on the Ti10Mo8Nb sample before the UFC quantization process described in the methodology.

The corrosion resistance of the Ti10Mo8Nb alloy, according to data seen in Figure 1, was adequate and congruent with information from the scientific literature for titanium alloys. Silva (2017) analyzed the corrosion resistance of commercially pure titanium and the Ti30Ta alloy, and observed greater resistance of the alloy, with passive current density values of  $1.3 \cdot 10^{-5}$  A/cm<sup>2</sup> and dissolution potential of 1.5 V, while commercially pure titanium had a passive current density of  $1.66 \cdot 10^{-4}$  A/cm<sup>2</sup> and a dissolution potential of 1.0 V. Zhang et al. (2021) studied the electrochemical behavior of Ti6Al4V alloys fabricated by the laser solid forming process. There was the formation of a passive region for the Ti6Al4V alloys at

1.58·10<sup>-5</sup> A/cm<sup>2</sup> and the dissolution potential was less than 1.5V.

The Ti10Mo8Nb alloy presented corrosion resistance very close to the Ti30Ta and Ti6Al4V alloys. All alloys are stronger than commercially pure titanium. The stability of the passive layer of the Ti10Mo8Nb and Ti30Ta alloys is greater than the others, occurring from 1.5 V. Among the materials compared, commercially pure titanium is the one with the lowest solidity of the passive layer, with a dissolution potential of 1.0 V. Ti6Al4V alloys presented intermediate values.

Many factors affect corrosion resistance, from experimental factors, such as the speed at which the potential and temperature vary, to inherent characteristics of the material, among which we can highlight the structure and composition (Silva, 2017). However, the contribution of the type of structure to corrosion resistance is very small when compared to the influence related to the composition. In this case, a greater resistance of the Ti10Mo8Nb alloy was expected when compared with Ti-cp, since Nb is an element with high resistance to corrosion. The greater corrosion resistance when compared to Ti-cp is evident, as the experimental alloy has lower current density and greater dissolution potential.

Few studies have studied the corrosion resistance of the Ti-Mo-Nb system and only the article by Chelariu et al. (2014) analyzed the Ti10Mo8Nb alloy. However, direct comparison of results is hampered, since most authors use Ringer's solution as the electrolyte. In the case of the research involving the Ti10Mo8Nb alloy, developed by Chelariu, an aqueous solution of NaCl (0.9% m) was used. The authors compared the corrosion resistance of several alloys in the Ti-Mo-Nb system, and observed an improvement in results with increasing Nb content, concluding that the presence of Nb in the oxide layer in concentrations between 8 and 16% m/ m, was more efficient in preventing electron transfer, which led to an increase in the corrosion resistance of these alloys when compared to the Ti12Mo alloy (Zhao et al., 2021).

Another study involving alloys from the Ti-Mo-Nb system was De Almeida et al. (2014), but in this study, the Ti10Mo8Nb alloy was not investigated. The authors compare the alloys Ti10Mo20Nb and Ti12Mo13Nb with the alloy Ti6Al4V in Ringer's solution. Analysis by potentiodynamic polarization led to the conclusion of greater corrosion resistance of Ti-Mo-Nb alloys, with an improvement in the result with increasing Nb content ( De Almeida, 2014).

Regarding the structure of the alloy, observed in Figure 2, small blackish precipitations in the image possibly indicate the presence of regions with a greater richness of Ti molecules. Chen et al. (2021) and Zhu et al. (2020) also observed similar blackish precipitation in the SEM images of their bulk alloy composite of TiMoNbZr and TiMoNb, respectively. Also, in their studies, they also observed a typical equiaxed conformation of crystals, with a grain size between 160-200 nm.

Furthermore, in relation to biocompatibility tests, based on the evaluation of bacterial proliferation, the result of the alloy was promising. Such an assessment is relevant as an indication of the possible emergence of an inflammatory and infectious process after surgery due to the formation of biofilm on the implant. The result, presented in the histogram in Figure 3, indicates that there is a higher concentration of colony-forming units in Ti-cp when compared to Ti10Mo8Nb for the bacteria *Staphylococcus aureus*. Therefore, an improved property of Ti10Mo8Nb alloy as an inhibitor of bacterial biofilm formation is observed.

With the established results, it can be argued that the Ti10Mo8Nb alloy, which until now has been little explored in the literature regarding its corrosion profile, presents superior corrosion resistance to that of Ti-cp, as well as being suitable for other more commonly used Ti alloys, such as Ti30Ta and Ti6Al4V. Added to this, there is the biocompatible profile and reduced bacterial proliferation of the Ti10Mo8Nb alloy when compared to Ti-cp. This information corroborates previous results of the alloy, which indicate mechanical and microhardness characteristics superior to other Ti alloys (Capellato et al., 2022). Therefore, the alloy presented in this study has potential and advantageous properties to make it applicable in the area of medical implants in orthopedics and dentistry.

## 4. Conclusion

The corrosion resistance property of Ti10Mo8Nb alloy was evaluated in this study. The importance of such analysis was considered high for the appropriate proposition of new alloys with optimized characteristics for applications in orthopedics and dentistry. Thus, Ti10Mo8Nb showed greater corrosion resistance than commercially pure Ti. Its grain structure was compatible with Ti alloys. The alloy also showed a significant reduction in bacterial proliferation (12.3%) in its structure. Thus, Ti10Mo8Nb presents itself as potential for use in the biomedical area.

## Acknowledgments

Partial financial support for this work was provided by the Brazilian federal government and the National Council for Scientific and Technological Development (CNPq) through Award Number 201271/2010-9 and Fapesp 2014/14533-3.

## References

- Apiwantanakul, N. & Chantarawatit, P-O. (2021). Cytotoxicity, genotoxicity, and cellular metal accumulation caused by professionally applied fluoride products in patients with fixed orthodontic appliances: a randomized clinical trial. *Journal Of The World Federation of Orthodontists*. 10(3), 98-104.
- Capellato, P., Vilela, F. B., Fontenele, A. H. P., Silva, G., Silva, K. B., Carobolante, J. P. A., Bejarano, E. G. M., Melo, M. L. N. M., Claro, A. P. R. A. & Sachs, D. (2022). Evaluation of Microstructure and Mechanical Properties of a Ti10Mo8Nb Alloy for Biomedical Applications. *Metals*. 12(7), 1065-77.
- Chelariu, R. et al. (2014). Metastable beta Ti-Nb-Mo alloys with improved corrosion resistance in saline solution. *Electrochimica Acta*. 137, 280-9.
- Chen, C., X.Y., Ji, X., Liang, X., Hu, Y., Cai, Z., Liu, J. & Tong, Y. (2021). Effects of Zr Content on the Microstructure and Performance of TiMoNbZrx High-Entropy Alloys. *Metals*. 11(8), 1315-21.
- De Almeida, L. H. et al. (2014). Corrosion resistance of aged Ti-Mo-Nb alloys for biomedical applications. *Journal of Alloys and Compounds*. 615, S666-S669.
- Dixon, A. (2022). The United Nations Decade of Healthy Ageing requires concerted global action. *Nature Aging*. Centre for Ageing Being, Londo UK.
- Dogra, S., Dunstan, D. W., Sugiyama, T., Stathi, A., Gariner, P. A. & Owen, N. (2022). Active Aging and Public Health: Evidence, Implications, and Opportunities. *Annual Reviews*. (43), 439-59. University of Ontario Institute of Technology, Faculty of Health Sciences.
- Gericke, L., Fritz, A., Osterhoff, G., Josten, C., Pieroh, P. & Höch, A. (2021). Percutaneous operative treatment of fragility fractures of the pelvis may not increase the general rate of complications compared to non-operative treatment. *European Journal Of Trauma And Emergency Surgery*. 48(5): 3729–35. doi: 10.1007/s00068-021-01660-w. Gil, A. C. (2017). Como elaborar projetos de pesquisa. (6ed.) Editora Atlas.
- Gu, D., Anreev, K. & Dupre, M. E. (2021). Major Trends in Population Growth Around the World. *China Cdc Weekly*. 3(28), 604-13. Chinese Center for Disease Control and Prevention.
- Guo, H., Jiang, J., Li, Y., Liu, M. & Han, J. (2022). An Aging Giant At The Center of Global Warming: Population Dynamics and Its Effect on CO2 Emissions in China. *Research Square*. 1-26. East China Norma University.
- Li, J., Zhou, P., Attarilar, S. & Shi, H. (2021). Innovative Surface Modification Procedures to Achieve Micro/Nano-Graded Ti-Based Biomedical Alloys and Implants. *Coatings*. 11 (6), 647-55.
- Massari, L., Benazzo, F., Falez, F., Perugia, D., Pietrogrande, L., Setti, S., Osti, R., Vainti, E., Aienti, E., Ruosi, C. & Cadossi, R. (2019). Biophysical stimulation of bone and cartilage: state of the art and future perspectives. *International Orthopaedics*. 43(3), 539-51.
- Montiel-Flores, E., Mejía-García, O. A., Ordoñez-Librado, J. L., Gutierrez-Valdez, A. L., Espinosa-Villanueva, J., Dorado-Martínez, C., Reynoso-Erazo, L., Tron-Alvarez, R., Rodríguez-Lara, V. & Avila-Costa, M. R. (2021). Alzheimer-like cell death after vanadium pentoxide inhalation. *Heliyon*. 7(8), 7856-69.
- Pereira A. S. et al. (2018). Metodologia da pesquisa científica. [free e-book]. Editora UAB/NTE/UFMS.
- Royhman, D., Pourzal, R., Hall, D., Lundberg, H. J., Wimmer, M. A., Jacobs, J., Hallab, N. J. & Mathw, M. T. (2021). Fretting-corrosion in hip taper modular junctions: the influence of topography and ph levels : an in-vitro study. *Journal Of The Mechanical Behavior Of Biomedical Materials*. 118, 104443-56.
- Silva, K. B. da et al. (2017). Corrosion Resistance After Mechanical Deformation of the Ti30Ta Experimental Alloy for Using in Biomedical Applications. *Materials Research*. 20(5), 1402-5.
- Toledano-Serrabona, J., Sánchez-Garcés, M. Á., Gay-Escoda, C., Valmaseda-Castellón, E., Camps-Font, O., Verdeguer, P., Molmeneu, M. & Gil, F. X. (2021). Mechanical Properties and Corrosion Behavior of Ti6Al4V Particles Obtained by Implantoplasty: an in vitro study. part ii. *Materials*. 14(21), 6519-25.

Zhang, Q., Duan, B., Zhang, Z., Wang, J. & Si, C. (2021). Effect of ultrasonic shot peening on microstructure evolution and corrosion resistance of selective laser melted Ti-6Al-4V alloy. *Journal Of Materials Research And Technology*. 11, 1090-9.

Zhao, R., Yang, R., Cooper, P. R., Khurshid, Z., Shavandi, A. & Ratnayake, J. (2021). Bone Grafts and Substitutes in Dentistry: a review of current trends and developments. *Molecules*. 26(10), 3007-18.

Zhu, W., Zhao, C., Zhang, Y., Kwok, C. T., Luan, J., Jiao, Z. & Ren, F. (2020). Achieving exceptional wear resistance in a compositionally complex alloy via tuning the interfacial structure and chemistry. *Acta Materialia*. 188, 697-710.